Photoluminescence properties of manganese activated calcium tungstate phosphors

M. J. Rao[a,b], K. S. R. Murthy[b], Ch. R. S. Kumar[b], B. P. Singh[b], G. S. V. R. K. Choudary[c], M. C. Varma[b,*]
[a]*Dr YC James Yen Government Polytechnic -Kuppam-517425, India*
[b]*Department of Physics, School of Science, GITAM (Deemed to be University), Visakhapatnam-530045, India*
[c]*Department of Physics, Bhavan's Vivekananda College, Sainikpuri, Secunderabad-500094, India*

This study presents the novel Mn doped $CaWO_4$ nanophosphors as an excellent alternatives of rare earth free materials for display application. The Mn doped $CaWO_4$ phosphor were characterized by various techniques, such as UV–Vis-DRS, Raman, PL analysis. Scheelite type tetragonal structure with space group I41/a has been confirmed. Rietveld analyses confirms the formation of single-phase solid solution. Lattice parameters for Mn free and Mn doped samples were calculated and observed that cell volume decreases after Mn incorporation. FTIR and Raman studies confirm the involvement of functional group and vibrational modes of vibration in the compound. Band gap values are estimated to be in the range of 4.2 to 4.33 eV with Mn doping. Photoluminescence study confirms the strong green emission at 450 and 515 nm (d-d transition in Mn^{2+}) after Mn doping. Also, it was observed that strong emission peak appears ~422 nm is mainly due to the electronic transition, $^1T_2 \rightarrow {}^1A_1$ in $[WO_4]^{2-}$ tetrahedron of CaWO4 host matrices. CIE study confirms that prepared nanophosphor exhibits strong blue colour after Mn incorporation. It can be employed as a potential material for blue phosphors in LEDs applications.

(Received February 11, 2024; Accepted May 24, 2024)

Keywords: $CaWO_4$, Band Gap (BG), Photoluminescence, Excitation and emission spectra, CIE diagrams

1. Introduction

Much attention has been paid to the production of phosphor materials, particularly materials having greater efficiency and high intensity on account of their effective uses in Field emission devices, Plasma display units, and light-emitting appliances [1–3]. Spherical and monodispersed (in micro or nano size) particles displaying non-agglomeration are pretty impressive for this kind of utility owing to their packing density and lower scattering of light [4]. Metal tungstates (XWO_4, X = Ca, Sr, Ba) exhibiting scheelite structure have assumed a vital role and attracted prominence due to its potential applications in different fields optical fibres, catalysis and humidity sensors [5- 8]. Calcium Tungstate, a self-activating phosphor, could give out blue emission of higher efficiency by tetrahedral complexes $[WO_4]^{2-}$ in the host lattices [9]. Alternative dopant materials are investigated to generate efficient luminescent materials as the cost and availability of rare-earth ions are highly restricted for synthesis.

White et al. [10] reported a bright green light emission in Mn-doped zinc silicate and phosphate in which Mn ions act as activators. Chan et al. [11] demonstrated an increase in the PL intensities in $LiZn_{1-x}PO_4:Mn_x$ phosphors, containing various concentrations of Mn ions, and later the intensities decreased in the wake of concentration quenching. Zhang et al. [12] attempted to explore the optical characteristics of Mn-doped XWO_4 where X = Ca, Sr, Ba nanorods and identified the increases substantially in photoluminescent potentiality due to Mn ions. It was observed that Mn-doped $CaWO_4$ nanorods produced 1.8 times greater luminescence intensity

* Corresponding author: cmudunur@gitam.edu
https://doi.org/10.15251/DJNB.2024.192.761

relative to pure $CaWO_4$ nanorods at the prominent peak positions at 502 nm. Regarding literature, it has been found that understanding the effect of Mn ions on luminescent properties of $CaWO_4$ is very much required, based on changes reported such as intensity increase/shift towards the blue region in Mn-doped luminescent substances. As the impact of Mn ions on $CaWO_4$ is essential to investigate in this work, manganese ions have been chosen as activator ions in $CaWO_4$ materials, and their influence on luminescent features has been undertaken presently.

2. Experimental procedure

Nanocrystalline $Ca_{1-x}Mn_xWO_4$ have been synthesized using $Na_2WO_4 \cdot 2H_2O$, $Ca(NO_3)_2 \cdot 4H_2O$ and $MnCl_2 \cdot 4H_2O$ and the synthesis procedure is given in [13]. Perkin Elmer LAMBDA 950 UV - VIS - NIR Spectrophotometer apparatus is availed, which is one state of art double beam, double monochromator spectrophotometer for clear understanding of UV-VIS spectrum and Band gap energy has been computed with the help of Kubelka and Munk procedure. Electronic transitions of molecules in a solution as well as in a solid-state material. Qualitative and Quantitative studies [13] of estimation of compounds are possible by this Non - Destructive method.

Photoluminescent excitation and emission [14 -15] measurements have been done, using Jasco spectrofluorometerFP-6300 with in range of 265 nm to 800nm for excitation spectra under emission wavelength of 255 nm and for recording emission spectra and excitation wavelength of 255 nm in range of 265 nm to 800 nm using Xe lamp, having shielded lamp house, 150-watt as light source and Silicon photodiode for excitation monochromator, Photomultiplier for emission monochromator detector.

3. Results and discussion

3.1. Lattice parameters

Lattice have been calculated by Rietveld refinement as implemented in MAUD software and are presented in earlier work [13]. The changes in the lattice parameters have been discussed based on Vegard law and the radii of ions of Mn^{2+}, Ca^{2+} are ± 0.83 ^{0}A, ±1 ^{0}A in octahedral sites and for W^{6+}, the radius is ± 0.42 ^{0}A in tetrahedral sites [17]. As the Mn^{2+} ion has a smaller radius, the unit cell constants are gradually reduced in solid state solutions with the increase in the concentration Mn^{2+} dopant quantity.

3.2. Particle size

Transmission electron micrographs are taken for all the samples, to understand the particle size and distribution with increasing Mn content in $CaWO_4$ materials. The following pictures show the particles, except for the $CaWO_4$ material all the Mn doped $CaWO_4$ show uniform particle size distribution.

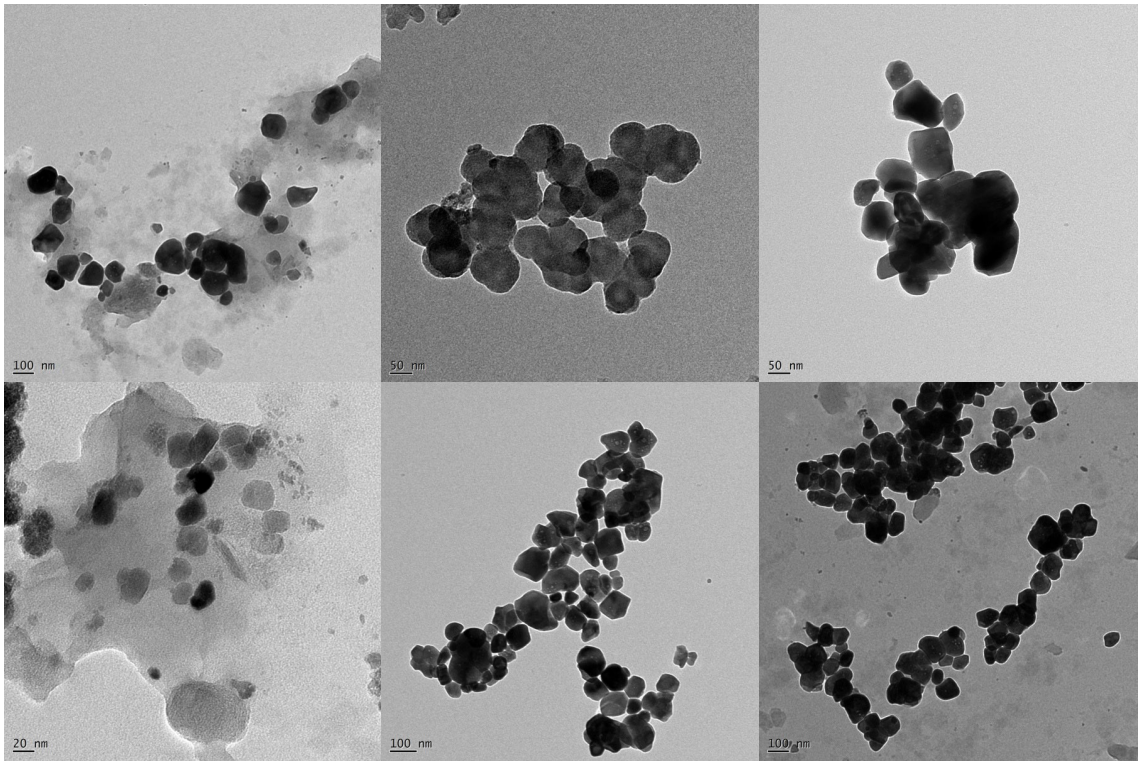

Fig. 1. (a) $CaWO_4$ TEM images; (b) $Ca_{0.98}Mn_{0.02}WO_4$TEM images; (c) $Ca_{0.96}Mn_{0.04}WO_4$ TEM image; (d) $Ca_{0.94}Mn_{0.06}WO_4$ TEM images; (e) $Ca_{0.92}Mn_{0.08}WO_4$ TEM images; (f) $Ca_{0.9}Mn_{0.1}WO_4$ TEM images

The above figures show the TEM images of the sample materials. The images illustrate all morphologies of the materials of different compositions. The particles are observed to be narrow sized and most of them are of nearly uniform sized according to the table of particle sizes. There is a formation of aggregated [15] microcrystals and these microcrystals are made of nanocrystals. The mechanism of the assembly of the crystals is regulated by interaction between paricles [16], following coalescence of octahedron crystals of nano order, like $CaWO_4$. The particle size has been calculated adopting the software Image J and considering Lorentz fit [14] for the distribution. The variation of particle size with Mn content is shown in the below table.

Table 1. Particle sizes of $Ca_{1-x}Mn_xWO_4$.

S.No	Sample	Particle size (nm)
1	$CaWO_4$	56.64
2	$Ca_{0.98}Mn_{0.02}$ WO_4	40.69
3	$Ca_{0.96}Mn_{0.04}$ WO_4	48.88
4	$Ca_{0.94}Mn_{0.06}$ WO_4	49.27
5	$Ca_{0.92}$ $Mn_{0.08}$ WO_4	71.87
6	$Ca_{0.9}Mn_{0.1}$ WO_4	70.96

Compared to the pure sample, the Mn^{2+} doped sample have a smaller particle size distribution. Hence, the effect of coalescence could result in reduction of particle size by doping in the host. The decrease in particle size is also explained as follows: During synthesis procedure, addition of calcium nitrate and manganese chloride solution to sodium tungstate, controls the

nucleation process which results less agglomeration of particles. On the other hand, on heating the prepared samples at 500°C will have high surface energy generates a bottle neck form by solid state diffusion process, which leads to agglomeration and particle growth. The larges differences in ionic radii between Ca^{2+} and Mn^{2+}, leads to a lattice distortion, which encourages a decrease in particle size. Hence, particle size reduces by doping due to a grain growth inhibition effect.

3.3. Raman spectra analysis

The vibrational modes in the Raman spectra of scheelite $CaWO_4$ are due to the vibrations of WO_4^{2-} tetrahedron against the Ca^{2+} (external modes) and the vibrations within WO_4^{2-} complexes in which Ca ions remains stationary (internal modes). Figure 2 shows the Raman modes of undoped CaWO4 sample.

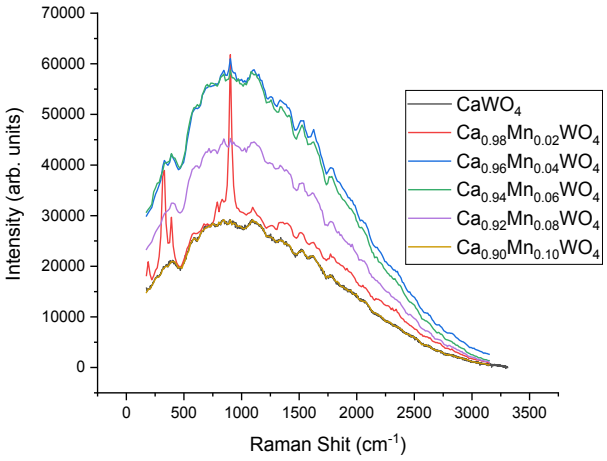

Fig. 2. Raman spectra of undoped and doped $Ca_{1-x}Mn_xWO4$.

Table 2. Vibrational Raman modes of $Ca_{1-x}Mn_xWO_4$ solid solution.

Sno	Specimen	Shift (cm^{-1})	Vib.Mode	Shift (cm^{-1})	Vib.Mode	Shift (cm^{-1})	Vib.Mode
1	$CaWO_4$	909.75	ν_1(Ag)	859.232	ν_3(Bg) , ν_2(Bg) ,B_g ,ν_3(Bg)	399.549 331.531, 357.352	ν_4(Bg), ν_3(Eg), Eg ,ν_4(Ag), ,B_g/Ag,ν_4(Bg), ν_2(Ag)
2	$Ca_{0.98}Mn_{0.02}WO_4$	903.568	ν_1(Ag)	849.848	ν_3(Bg) , ν_2(Bg) ,B_g ,ν_3(Bg)	324.172, 341.444	,ν_4(Ag), ,B_g/Ag,ν_4(Bg), ν_2(Ag)
3	$Ca_{0.96}Mn_{0.04}WO_4$	905.056	ν_1(Ag)	-	-	303.513	ν_4(Ag), ,B_g/Ag,ν_4(Bg), ν_2(Ag)
4	$Ca_{0.94}Mn_{0.06}WO_4$	902.304	ν_1(Ag)	826.301	ν_3(Bg) , ν_2(Bg) ,B_g ,ν_3(Bg)	323.861 337.8	ν_4(Ag), ,B_g/Ag,ν_4(Bg), ν_2(Ag)
5	$Ca_{0.92}Mn_{0.08}WO_4$	901.972	ν_1(Ag)	-	-	312.409 323.26	ν_4(Ag), ,B_g/Ag,ν_4(Bg), ν_2(Ag)

The Raman spectra are analysed and recorded in the wavenumber range of 100–1000 cm-1, as shown above. Table 3 lists their vibrational modes, as seen in the diagram above. The development of a covalent link between Manganese ions of doped material and oxygen ions of [WO4]2- complex anion is related to the change in Raman wavenumbers from CaWO4 to

Ca0.9Mn0.1WO4 solid solutions. Internal mode stretching (v3(F2)) and internal bending (v4(F2)) are only active at IR frequencies. The mechanism of stretching in the [WO4]2- tetrahedron group ions may be found to be induced by W – O resistant symmetric enlarging vibrations. In the Raman shift range of 900–1000 cm-1, there is only one Raman vibration mode, which is identified as v1(Ag) with varied quantities of the dopant, Mn2+ ions. For CaWO4 materials with varied quantities of Mn2+ atoms, the Raman vibration modes are 3(Bg), 2(Bg), 3(Bg), and Bg, respectively, in the range 820 – 900 cm-1. For solid solutions, the Raman vibration modes include 4(Ag), 2(Ag), 4(Bg), 4(Bg), Bg/Ag, Eg, and 3(Eg) within the Raman shift range of 300–400 cm-1. Small changes in the spectra created by the dopant, Mn2+, and distortions in the O-W-O bonds or O-Ca-O bonds are seen in the Raman forms. The substitution of Ca2+ ions by Mn2+ ions might explain the contact forces for [WO4] –[CaO8]-[WO4] bunch groups, order-disorder [18] of various levels of the structural composition of the lattice at short range. It's also possible that the reduction in the average size of crystals is connected to the narrowing of Raman peaks by lesser amounts.

3.4. Uv-vis spectra

Bandgap for all the samples has been determined using Kubelka and Munk method as described in earlier work [JETIR June 2019, Volume 6, Issue 6 2055-2059]. The observed bandgap for CaWO4 is further established using DFT calculations as implemented in Quantum Espresso and those are given in the earlier work [JETIR June 2019, Volume 6, Issue 6 2055-2059].

In general, the Kubelka and Munk equation [18] is given by

$$F(R_\infty) = \frac{(1 - R_\infty)^2}{2R_\infty} = \frac{k}{s}$$

R_∞ denotes the absolute reflectance, k shows absorption coefficient and s is scattering coefficient. $F(R_\infty)$ is generally known as remission or Kubelka – Munk (K-M) function.

The optical band space energy (Eg) of Mn ions doped $CaWO_4$ samples have been evaluated with the process, mooted by Kubelka and Munk [18]. According to knowledge of literature, leaving $PbMoO_4$ and $PbWO_4$, every remaining divalent metal molybdates, tungstates having tetragonal scheelite structure (alkaline earth metal molybdates and tungstates) display an absorption spectrum of optics, found to be regulated using absorption procedure directly (n = 1/2) [22-24].

Finally, by the remission function mentioned in equation along with the quantity $k = 2\alpha$, C_2 is a constant of proportionality, the modified Kubelka–Munk equation is as follows

$$[F(R_\infty)h\upsilon]^2 = C_2\left(h\upsilon - E_g\right)$$

Hence, calculating the $F(R_\infty)$magnitude using equation and drawing a curve of $[F(R_\infty)h\upsilon]^2$ against hυ made it possible to determine the E_{gap} of $CaWO_4$ and Mn doped $CaWO_4$ materials.

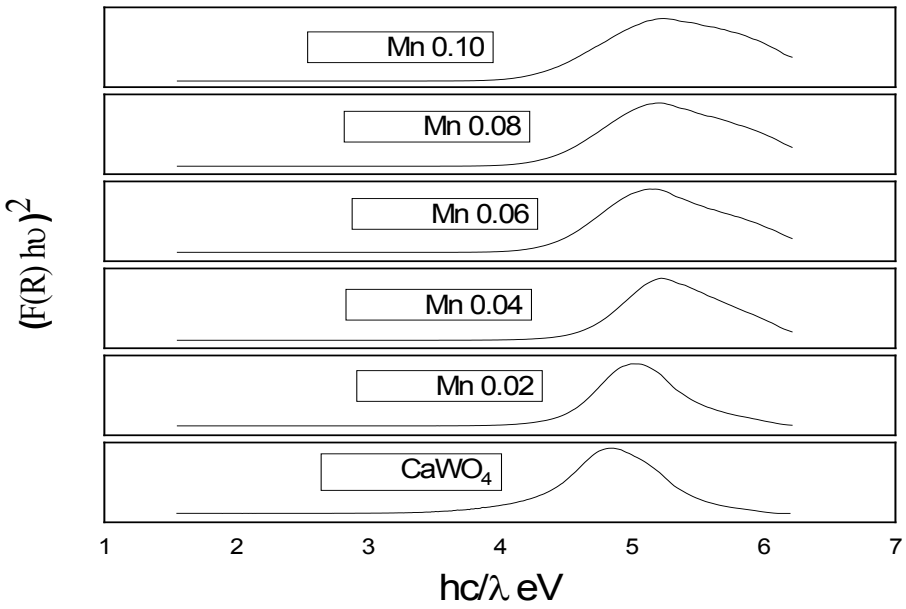

Fig. 3. Uv-Vis spectra of $Ca_{0.92}Mn_{0.08}WO_4$.

The estimated E_g (BG) values of all the samples are tabulated in the following table 3.

Table 3. Band gap energy values of solid solutions.

S.No.	Sample	Band Gap (eV)
1	$CaWO_4$	4.33 []
2	$Ca_{0.98}Mn_{0.02}WO_4$	4.50
3	$Ca_{0.96}Mn_{0.04}WO_4$	4.47
4	$Ca_{94}Mn_{0.06}WO_4$	4.30
5	$Ca_{0.92}Mn_{0.08}WO_4$	4.20

From the above table 3, it can be observed that for Mn ions content, x = 0.02, bandgap slightly increased and this can be attributed to sudden change in the electronic structure due to a decrease in the lattice constant. The changes observed in UV-Visible spectra show that doping of Mn^{2+} provides weaker absorption in the ultraviolet region, indicating a decrease in the energy required for exciting the valence band electron to the conduction band. The reported band gap value of $MnWO_4$ is 2.79 eV [25] which is less than that of $CaWO_4$ (4.33 eV observed in the present study or that reported value of 4.39 eV [26] and supports the observed variation in bandgap of Mn^{2+} ions doped solid solution, $CaWO_4$. The decrease in lattice constant values may develop slight distortion of scheelite structure with the doping of manganese ions (Mn^{2+}), which may lead to the formation of intermediary energy levels in the conduction band, as discussed by Lourdes Gracia et al [27]. In turn, it decreases the band gap between the valence band and conduction band of these solid solutions.

3.5. Photoluminescence (PL) study

The photoluminescence results of the solid-state solutions, $Ca_{1-x}Mn_xWO_4$ have been shown below in the form of excitation and emission spectra.

3.5.1. Excitation spectra

The excitation of the materials has been carried out, and the relevant spectra are obtained. The excitation wavelengths of solid solutions, Calcium Tungstate and Calcium Tungstate, activated with Mn^{2+} ions are illustrated in the table 4. The solid solutions are excited with

wavelengths, which are in the order of increase. The PL spectra are affected using concentration of the dopant, Mn^{2+} ions and host solid solution, Calcium Tungstate. The excitation and emission, describing luminescence characteristics of the materials, can be understood by the order and disorder, taking place in the samples, i.e. structural qualities.

The transition of $^4T_1$-$^4A_1$ in Mn^{2+} ions results in PL spectra (Emission and Excitation) of Calcium Tungstate, observed in the blue region of the EM spectrum. The intensity increases in the excitation wavelength range, 320-375 nm with the rise concentration of Mn^{2+} ions. The intensity decreases in the range of excitation wavelength, 375- 400 nm whereas it increases in the range 400-425 nm when the quantity of Mn^{2+} ions grows. The ranges of excitation wavelengths, 425-450 nm and 450-475 nm indicate fall and spike in intensity one after another & later decreases after 475 nm up to 525 nm.

The excitation spectra report that the existence of Mn^{2+} ions in the host lattice would serve as emission agent. The main peaks of excitation curves reveal the excitation wavelengths at 375 nm and 400 nm for all samples, belonging to UV region. This can be noticed because of disintegration of energy states as per the strength of the field with the introduction of free $3d^n$ transition metal ions, ie Mn^{2+} ions into the host lattice. The excitation spectra depict that the PL spectra of the materials with dopants are affected by the structural features of these materials and the surrounding host material. Due to concentration quenching, the PL intensity decreases with higher concentration of Mn^{2+} ions.

In respect of excitation spectra (270 nm), the peaks at 350 nm, 400 nm, 450 nm, 460 nm, 475 nm were observed. These peaks were attributed to $^6A_1(S) \rightarrow {}^4A_1$, $^4E(4G)$, $^6A_1(S) \rightarrow {}^4T_2(4G)$ and $^6A_1(S)$) $\rightarrow {}^4T_1(G)$, which are d – d transitions of Mn^{2+} ions. The shift in peak positions, when compared with Mn^{2+} ions in other materials can be found to be due to delocalization of Mn^{2+} ions in the host lattice [28 – 31]

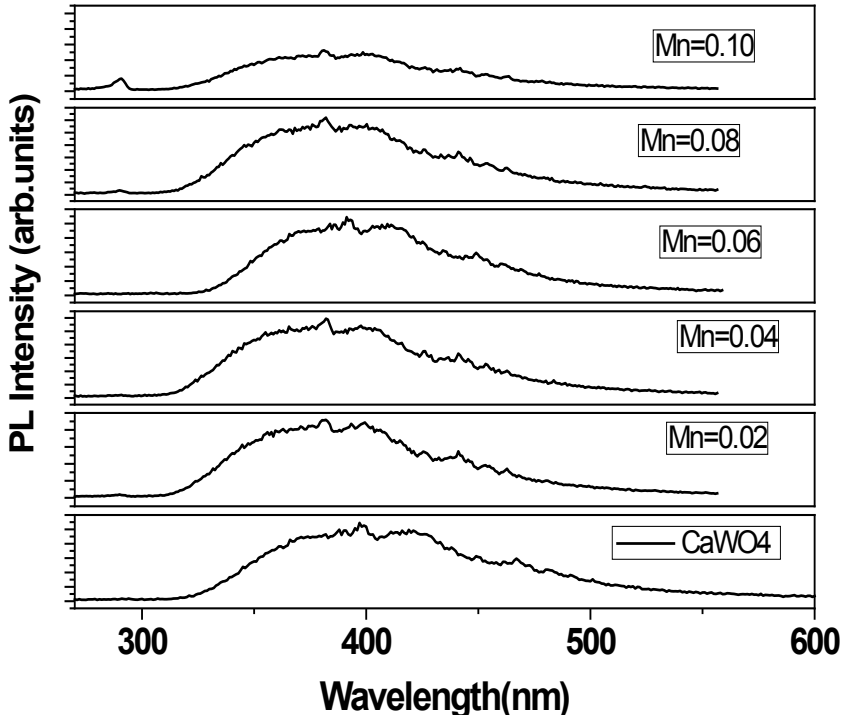

Fig. 4. $Ca_{0.92}$ $Mn_{0.08}WO_4$ sample.

Table 4. Excitation wavelengths.

Mn^{2+} ions content	Excitation wavelengths						
0	356.53	395.67	421.51	451.20	-	-	-
0.02	358.06	393.89	435.11	476.84	472.51	513.63	-
0.04	356.75	392.51	433.9	455.63	469.42	510.38	-
0.06	358.51	392.47	424.02	468.41	471.62	480.61	-
0.08	358.86	393.35	428.4	476.8	513.11	470.5	-

3.5.2. Emission spectra

The PL emission peak was found to be around 422 nm (blue region) and the emission was due to the transition, $^1T_2 \rightarrow {}^1A_1$ in $[WO_4]^{2-}$ excited complexes [32]. There could be an accumulation of Mn^{2+} ions at the surface in heavily doped Calcium Tungstate nanoparticles. In case of pure Calcium Tungstate nanoparticles, only one peak was observed around 450 nm and could be attributed to $CaWO_4$ emission [33]. However, in case of Mn^{2+} ions doped $CaWO_4$ nano particles, the emission spectra show 2 peaks, according to the Table 5, centred at 350 nm and 515 nm. The peak, corresponding to 515 nm is due to d – d transition of Mn^{2+} ions. It can be drawn from emission spectra that with the increase in concentration of Mn^{2+} ions, the intensity slowly increases and at around 515 nm, it reaches a maximum value. The decrease in intensities, represented by peaks can be due to accumulation of more number of Mn^{2+} ions on the surface of nano particles of $CaWO_4$ [34]

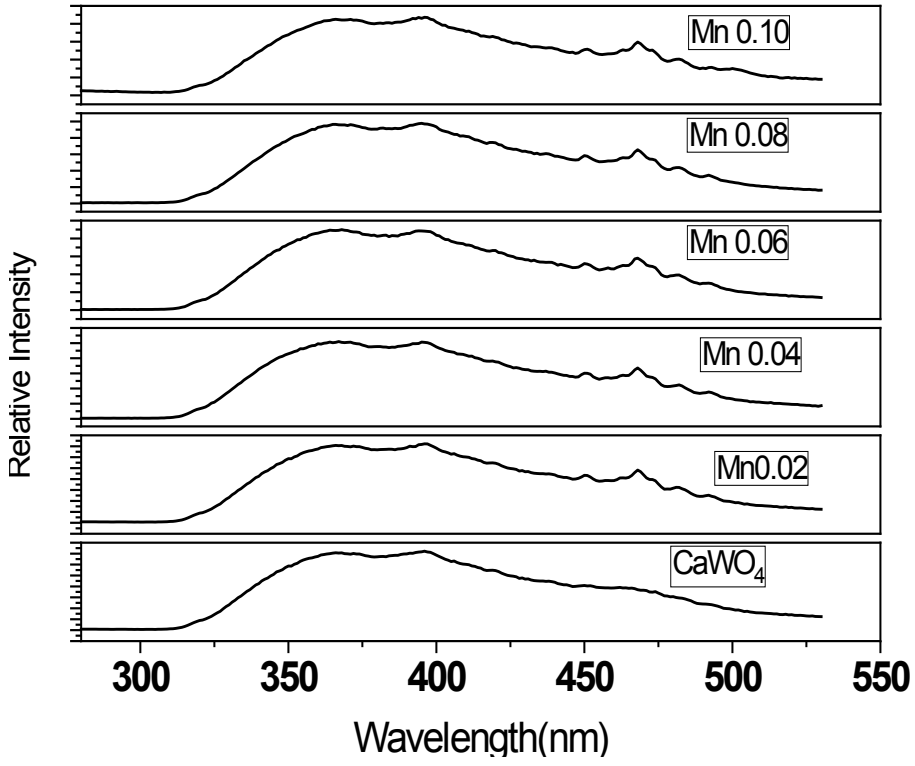

Fig. 5. $Ca_{0.92}Mn_{0.08}WO_4$ sample.

Table 5. Emission peak wavelengths.

Sample	Emission peak wavelengths (nm)						
$CaWO_4$	330	352	421	-	-	481	-
$Ca_{0.98}Mn_{0.02}WO_4$	327	346	415	451	469	483	507
$Ca_{0.96}Mn_{0.04}WO_4$	330	347	417	453	469	483	507
$Ca_{0.94}Mn_{0.06}WO_4$	327	347	417	451	469	483	507
$Ca_{0.92}Mn_{0.08}WO_4$	330	345	-	452	469	483	507

3.5.3. CIE diagrams

The Commission Internationale d I'Eclairge (CIE) chromaticity diagrams 1931 of undoped, Mn doped samples are shown in figure 6.

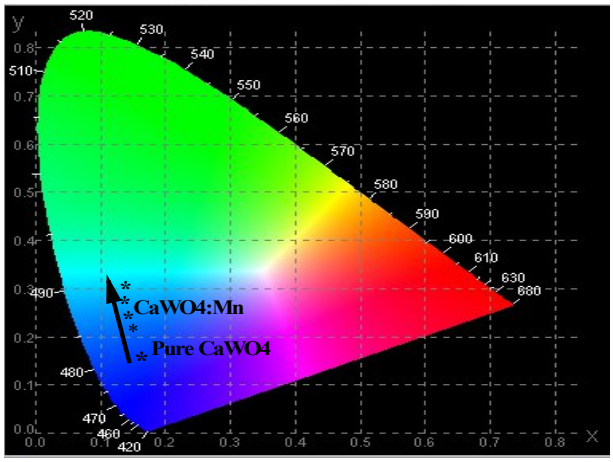

Fig. 6. CIE diagram of $CaWO_4$ and Mn doped $CaMnWO_4$

Table 6. Purity of solid solutions, $Ca_{1-x}Mn_xWO_4$.

Sample	x	y	Colour Purity
$CaWO_4$	0.1603	0.1425	79.8%
$Ca_{0.98}Mn_{0.02}WO_4$	0.1303	0.2024	84.0%
$Ca_{0.96}Mn_{0.04}WO_4$	0.1178	0.2859	81.4%
$Ca_{0.94}Mn_{0.06}WO_4$	0.1248	0.2445	82.0%
$Ca_{0.92}Mn_{0.08}WO_4$	0.1259	0.2366	82.3%

The colour coordinates of different samples of Calcium Tungstate with different amounts of dopant, ie Mn^{2+} ions are depicted in the Table 6. The pure Calcium Tungstate phosphor exhibits blue colour. When the amount of dopant increases from 0.02 to 0.06, the samples have been observed to emit light in blue –greenish colour under excitation. As the quantity of dopant, Mn^{2+} ions becomes 0.08, the material has been noticed to produce green whitish light in agreement with CIE diagrams of samples. Therefore, it can be understood that by varying the amounts of dopants in the sample in steps of 0.01 from 0.08 white light emission may be possible.

4. Conclusions

The modes of vibration were noticed with the help of Raman spectroscopy and were in good agreement with XRD analysis and FTIR published in previous work [13]. The bandgap studies were performed to examine and investigate the optical properties of Calcium Tungstate materials by UV-Vis spectra and Diffuse Reflectance Spectroscopy. The PL spectra are affected by quantities of the dopant, Mn ions and host material, Calcium Tungstate. The order could clearly interpret the excitation and emission, illustrating luminescence characteristics of the materials and disorder taking place in the samples, i.e. structural characteristics.

The transition of $^4T_1$-$^4A_1$ in Mn ions results into PL spectra (Emission and Excitation) of Calcium Tungstate, observed in the blue region of EM spectrum. The excitation spectra show that PL spectra of materials with dopants get affected utilizing structural features of the materials and the surrounding host material. The shift in peak positions can be attributed to delocalization of manganese ions in the host lattice.

The decrease in intensities, illustrated by peaks in emission spectra, can be due to the accumulation of more manganese ions on the surface of nano particles of Calcium Tungstate. CIE diagrams point to the fact of continuous substitution of Manganese ions in place of Calcium ions with the rise in the amount of Manganese ions and causes increase in maximum green whitish PL emission due to transition of $^4T_1$-$^4A_1$ in Mn ions and a suitable quantity of dopant may result in efficient white light emission.

Acknowledgements

One of the authors (G.S.V.R.K. Choudary) is grateful to UGC-SERO, Hyderabad, India for granting the financial assistance in order to purchase the equipment, utilized in the synthesis through Minor Research Project No. FMRP – 6812 (2017 – 18) (SERO/UGC). Authors are also thankful to the Department of Physics, GSS, GITAM (Deemed to be University) for providing the DSC-TGA facility sanctioned through DST-FIST, India, for providing infrastructural facilities-(equipment) through No.SR/FST/PSI-194/2014 Dated: 21st July 2015.

References

[1] R. C. Jin, Y. W. Cao, C. A. Mirkin, K. L. Kelly, G. C. Schatz, J. Zheng, Science 294,190 (2001); https://doi.org/10.1126/science.1066541

[2] M. Li, H. Schnablegger, S. Mann, Nature 402, 393 (1999); https://doi.org/10.1038/46509

[3] M. A. El-Sayed Accounts of Chemical.Research. 34, 257 (2001); https://doi.org/10.1021/ar960016n

[4] R. Liu, J. F. Liu, G. B. Jiang, Chemical Communications 46, 7010 (2010); https://doi.org/10.1039/c0cc02466j

[5] X. G.Peng, L. Manna, W. Yang, J. Wickham, E. Scher, A. Kadavanich, A. P. Aliviisatos, Nature 404, 59 (2000); https://doi.org/10.1038/35003535

[6] G. Jia, K. Liu, Y. H. Zheng, Y. H. Song, H. P. You, Crystal Growth and Design 9, 3702 (2009); https://doi.org/10.1021/cg9004104

[7] Q. A. Zhang, W. Y. Li, C. Moran, J. Zeng, J. Y. Chen, L. P. Wen, Y. N. Xia, Journal of American Chemical Society 132, 11372 (2010); https://doi.org/10.1021/ja104931h

[8] Y.G. Su, L. P. Li, G. S. Li, Chemistry of Materials 20, 6060 (2008); https://doi.org/10.1021/cm8014435

[9] A. Phuruangrat, T. Thongtem, S. Thongtem, Journal of Experimental Nanoscience 5, 263 (2010); https://doi.org/10.1080/17458080903513276

[10] J. W. Hess Jr., J. R. Sweet, W. B. White, Journal of Electrochemical Society 121, 142 (1974); https://doi.org/10.1149/1.2396809

[11] T. S. Chan, R. S. Liu, I. Baginskiy, Chemistry of Materials 20, 1215 (2008); https://doi.org/10.1021/cm7028867

[12] F. Zhang, Y. Yiu, M. C. Aronson, S. S. Wong, Journal of Physical Chemistry C, 112 14816 (2008); https://doi.org/10.1021/jp803611n

[13] M. Jaganadha Rao, K. S. R. Murthy, Ch. Ravi Shankar Kumar, Anjali Jha, G. S. V. R. K. Choudary, M. Chaitanya Varma Asian Journal of Chemistry 32, 49 (2020); https://doi.org/10.14233/ajchem.2020.22199

[14] Rasband WS. ImageJ, U.S. National Institute of Health, Bethesda, USA, image.nih.gov/ij/1997-2012

[15] Wanbiao Hu, Wenming Tong, Liping Li, Jing Zheng, Guangshe Li, Physical Chemistry Chemical Physics, 13 , 11634 (2011); https://doi.org/10.1039/c0cp02153a

[16] Xiaomin Yang, Yuhong Wang, Na Wang, Suli Wang, Guijun Gao Journal of Material Science : Materials in Electronics 25, 3996 (2014); https://doi.org/10.1007/s10854-014-2119-4

[17] Qiang Yu, Hengyi Lei, Guangwei Yu, Xin Feng, Zhaoxu Li, Zhicheng Wu, Chemical Engineering Journal, 155 , 88 (2009); https://doi.org/10.1016/j.cej.2009.07.010

[18] P. Kubelka, F. Munk, Ein Beitrag zur Optik der Farbanstriche, Z. Technical Physics, 12, 593 (1931)

[19] J. Tauc, R. Grigorovici, A. Vancu, Phyica.Status Solidi 15, 627 (1966); https://doi.org/10.1002/pssb.19660150224

[20] J. Tauc, Menth, States in the Gap, Journal of Non Crystaline Solids, 810, 569 (1972); https://doi.org/10.1016/0022-3093(72)90194-9

[21] J. Tauc, Materials Research Bulletin, 3, 37 (1968); https://doi.org/10.1016/0025-5408(68)90023-8

[22] Thongtem, T., Kungwankunakorn, S., Kuntalue, B., Phuruangrat, A., Thongtem, S, 2010. Journal of Alloys and Compdounds 506 475 (2010); https://doi.org/10.1016/j.jallcom.2010.07.033

[23] Jira Janbua, Jitkasem Mayamae, Supamas Wirunchit, Rattanai Baitahe, Naratip Vittayakorn. RSC Advances 5 19893 (2015); https://doi.org/10.1039/C4RA15064C

[24] Zhang Y., Holzwarth N. A. W., Williams R. T., Physical Review B 57, 12738 (1998); https://doi.org/10.1103/PhysRevD.57.3749

[25] Swagata Dey, Rebecca A. Ricciardo, Heather L. Cuthbert, Patrick M. Woodward Inorganic Chemistry 53, 4394 (2014); https://doi.org/10.1021/ic4031798

[26] C Nagarajan, S Monesh Kumar, R Annie Sujatha, K. Mani Rahulan, Angeline Little Flower IOP Conference Series: Material Science Engineering 1219, 012008 (2022); https://doi.org/10.1088/1757-899X/1219/1/012008

[27] Lourdes Gracia et al., Journal of Applied Physics 110, 043501 (2011).

[28] Wei Chen, Ramasami Sammynaiken, Yining Huang, Jan-Olle Malm, Reine Wallenberg, Jan-Olov Bovin, Valéry Zwiller, Nicholas A. Kotov, Journal of Applied Phyics 80 1120 (2001); https://doi.org/10.1063/1.1332795

[29] R Ajay Kumar, M. V. V. K. Srinivas Prasad, G. Kiran Kumar, M. Venkateswarlu Ch. Rajesh, Physica Scripta 94, 115806 (2019); https://doi.org/10.1088/1402-4896/ab242a

[30] Ch. Rajesh, Amit D. Lad, Ajit Ghangrekar, Shailaja Mahamuni, Journal of Solid state Communications 148, 435 (2008); https://doi.org/10.1016/j.ssc.2008.09.022

[31] P. Suneeta, R.A. Kumar, M.V. Ramana, G.K. Kumar, A. Chatterjee, C. Rajesh, Physica Scripta 95, 035806 (2020); https://doi.org/10.1088/1402-4896/ab4d2a

[32] A. Phuruangrata, T. Thongtema T, S. Thongtema, Journal of Experimental Nano science 5, 263 (2010).

[33] R. Grasser, A. Scharmann, K.-R. Strack, Journal of Luminescence, 27, 263 (1982); https://doi.org/10.1016/0022-2313(82)90004-7

[34] Mahamuni, Shailaja, Amit D. Lad, Shashikant Patole, J. Physical Chemistry C 112, 2271 (2008); https://doi.org/10.1021/jp076834m